Liquid Crystals

DOI: 10.1002/ange.201300658

A General Method for the Enantioselective Formation of Helical Nanofilaments**

*Takahiro Ueda, Shiori Masuko, Fumito Araoka, Ken Ishikawa, and Hideo Takezoe**

Chirality has been an important subject in chemistry since Pasteur demonstrated the existence of molecules that were mirror images of each other.[1] Indeed, chirality has proven to be important in the fields of biology and pharmacy as well.[2] In the past, single enantiomers have been made by using asymmetric catalysis[3,4] and enantiomeric separation.[5] However, almost all methods rely on the use of chiral molecules. Recently, the development of asymmetric reactions that do not use chiral molecules is attracting lot of attention. In this respect, bent-core liquid crystals (BCLCs)[6–8] are very interesting because layer chirality occurs in nonchiral molecular systems as a result of the tilt of polar-ordered molecules from the normal of the smectic layer,[9] and is coupled with conformational molecular chirality.[10] Moreover spontaneous deracemization to give large chiral domains occurs particularly in the helical nanofilament (HNF) B4 phase because of negative splay elastic constants.[7–12] Each macroscopic chiral domain consisting of HNFs exhibits high optical activity.[11,13–15] The formation of a helical structure in the B4 phase suggests that the chirality can be controlled, because in many other organic systems the handedness of the helical structure has been controlled by external chiral sources, such as circularly polarized light,[16,17] vortex flow,[18–20] and helicity memory induced by chiral molecules.[21]

Previously, we used five different methods to control the chirality of the B4 phase and successfully obtained almost 100% *ee* with some of them. These methods are: 1) the introduction of chiral analogues,[22] 2) the use of a chiral surface,[23] 3) irradiation of photoisomerizable molecules with circularly polarized ultraviolet (UV) light,[24] 4) the use of twisted nematic (TN) director orientation,[25] and 5) growth from a chiral phospholipid layer.[26] Methods 2 and 5 both involve the use of a chiral surface, however, with the former only 10% *ee* was attained, whereas with the latter almost 100% *ee* was attained. The difference originates from the absence (method 2) and presence (method 5) of a temperature gradient. Contrary to the use of chiral dopants in method 1 and chiral surfaces in methods 2 and 5, methods 3 and 4 do not require any chiral species and have the added advantage that they work on bulk samples. However, the phase sequences of the compounds used for methods 3 and 4 are restricted by necessary phase sequences, that is, a fluid smectic phase (method 3) and a nematic (N) phase (method 4) that occur at higher temperatures to the B4 phase. Namely, a gradual phase transition from fluid smectic phases to the B4 phase under circularly polarized UV irradiation triggers repeated photoisomerization, whereas UV irradiation in the B4 phase is not an effective method to control chirality. Only one example of method 4 is known[25] because of the lack of compounds showing the N–B4 phase transition. Herein, we present a general method based on method 4 that is applicable for compounds that display no N phase but exhibit the B4 phase. The method is very simple: mixing a bent-core compound showing the B4 phase with a compound exhibiting the N phase realizes the phase sequence of N–Bx, where we use Bx to distinguish the microphase separated B4/N state from the B4 phase. Conveniently, other phases, such as B1, B2, and B3, which often occur between the isotropic (Iso) and the B4 phases, readily disappear by the introduction of a rod-like compound.[13,14]

We prepared three mixtures consisting of bent-core and rod-like compounds that display the N phase at higher temperatures to the Bx phase. The chemical structures of each component are shown in Scheme 1. We used two bent-core compounds that show the B4 but no N phase: 1,3-phenylenebis[4-(4-8-alkoxyphenyliminomethyl)-benzoates] (P8-O-PIMB; Iso–B2–B3–B4)[27] and α,ω-bis(4-alkoxyazobenzene-4′-carbonyloxy)alkene (12OAzo5AzoO12; Iso–SmC_A–B4).[28] For rod-like compounds, we used *n*-pentylcyanobiphenyl (5CB; Iso–N–Cryst), 4′-cyano-(1,1′-biphenyl)-4-yl-4-pentylbenzoate (5PCB; Iso–N–Cryst), and ZLI-2293 (a cyano-type nematic mixture from Merck; Iso–N). We made three

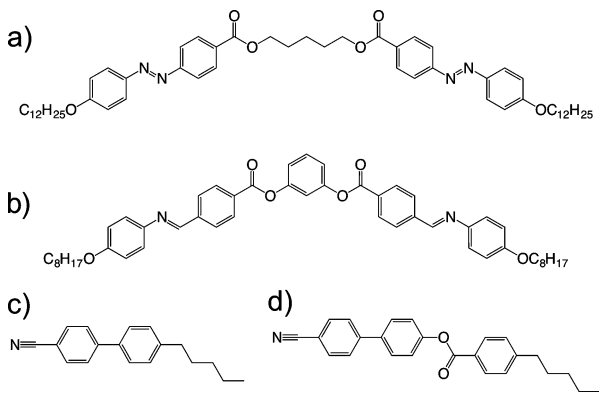

Scheme 1. Chemical structures of bent-core and rod-like components of the three mixtures: a) 12OAzo5AzoO12, b) P8-O-PIMB, c) 5CB, and d) 5PCB. Commercially available ZLI-2293 (Merck) was also used.

[*] T. Ueda, S. Masuko, Dr. F. Araoka, Prof. K. Ishikawa, Prof. H. Takezoe
Department of Organic and Polymeric Materials
Tokyo Institute of Technology
O-okayama, Meguro-ku, Tokyo 152-8552 (Japan)
E-mail: takezoe.h.aa@m.titech.ac.jp

[**] The authors are grateful to DIC and Merck for supplying 12OAz5AzO12 and ZLI2293.

Supporting information for this article is available on the WWW under http://dx.doi.org/10.1002/anie.201300658.

mixtures (mixture 1: 12OAzo5AzoO12 (40 wt%) and ZLI-2293 (60 wt%); mixture 2: 12OAzo5AzoO12 (40 wt%), 5CB (35 wt%), and 5PCB (25 wt%); mixture 3: P8-O-PIMB (50 wt%) and 5PCB (50 wt%)). The phase sequences of these mixtures are listed in Table 1. Herein, we will show the data obtained for mixture 1; the data obtained for mixtures 2 and 3 are shown in the Supporting Information.

Table 1: Mixing ratios of bent-core and rod-like molecules in the mixtures used and their phase sequences.

Mixture	Bent-core	Rod-like	Phase sequence
Mixture 1	12OAzo5AzoO12	ZLI2293	Iso 86 °C N 62 °C Bx(B4+N)
Mixture 2	12OAzo5AzoO12	5CB + 5PCB	Iso 98 °C N 69 °C Bx(B4+N) 22 °C Cryst
Mixture 3	P8-O-PIMB	5PCB	Iso 171 °C N 132 °C Bx(B4+N) 58 °C Cryst

To obtain TN cells we spin-coated glass substrates with surface agent AL1254 (JSR), baked the glass substrates, and then rubbed the surfaces in one direction. The sample thickness was less than 2 μm. Figure 1 shows the polarizing microscope images displaying the textures of the N and Bx phases in mixture 1 observed in a 2 μm thick cell with a twisted angle of $\theta = +60°$. Positive and negative rotations are defined here as clockwise and counterclockwise rotations of the rubbing direction on the upper surface with respect to the the lower surface, to make a left- and right-handed twist, respectively. The solid and dotted white arrows represent the polarization direction of polarizers located at the upper and lower sides of the cell, respectively and the solid and dotted red arrows represent the direction of rubbing on the upper and lower surfaces, respectively. Normally dark and bright states are shown in Figure 1a and b, respectively, thus demonstrating that the molecules form with a twist angle of 60°. After slowly cooling the TN cell to form the Bx phase, a dark low-birefringent texture was obtained under crossed polarizers (Figure 1c). Notably, the texture of the Bx phase in mixture 1 is preserved without crystallization for at least several months at room temperature.

Circular dichroism (CD) measurements (JASCO, J-720WI) were performed to confirm the occurrence of deracemization in the Bx phase. Figure 2a shows the UV/Vis absorption spectra of each component of mixture 1 in a quartz cell (cell thickness: about 0.8 μm). Figure 2b shows typical CD spectra of the Bx phase of mixture 1 in the TN cells with various twist angles (0° (antiparallel), −20°, −40°, −60°, +60°). A comparison of the absorption and CD spectra reveals that the CD signal at about 325 nm originates from helical nanofilaments formed by 12OAzo5AzoO12 molecules in the Bx phase, whereas the signal at about 280 nm originates from ZLI-2293 molecules. To investigate the origin of the CD signal, measurements were carried out by rotating cells about the normal of the cell surface. The signal intensity drastically changed with the rotation angle in a cell rubbed in the antiparallel direction, thus indicating that linear dichroism is the origin of CD signal (see the Supporting Information,

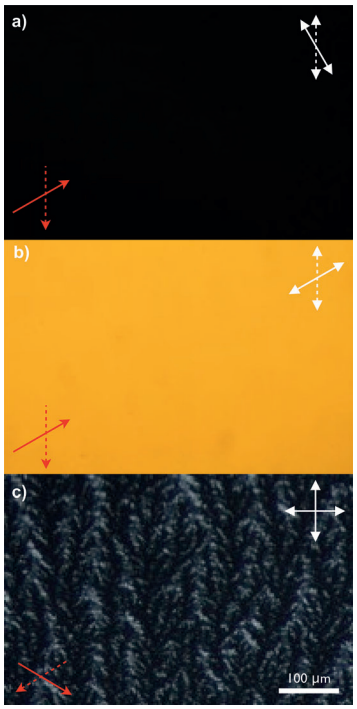

Figure 1. Optical photomicrographs of mixture 1 in the N (75 °C) and Bx (60 °C) phases. a) Normally dark state of a TN cell with a twist angle of +60°. b) Normally bright state of a TN cell with a twist angle of +60°. c) The formation of the Bx phase by slowly cooling the TN state under crossed polarizers. The Bx phase appears as a dark state. Slight brightness originates from the low birefringence of the B4 phase and optical rotatory power of the microphase separated B4 and TN structures. White and red arrows are directions of light polarization and rubbing, respectively. Solid and dotted lines distinguish these directions at upper and lower sides, respectively.

Figure S1a). In contrast, the variation of the CD signal at all rotation angles is marginal compared with the intense CD signal in twisted cells (see the Supporting Information, Figure S1b for a 40° twisted cell) particularly for the signal at 325 nm corresponding to HNFs, thus confirming the chirality origin of the CD signal. Large induced CD signals with mutual mirror images were observed for right- and left-handed TN cells (±60°), thus indicating successful control of the chirality of the helical nanofilament (Figure 2b). The intensity of the CD signal at 325 nm only moderately increases when the twist angle is increased from −20° to −60°. In contrast, the CD signal at 280 nm increases significantly with increasing twist angle. These experimental findings are closely related to the origin of the CD spectrum, which will be discussed after showing all data. To confirm that HNFs were formed across the whole cell, we measured the CD spectra for cells with a twist angle of −40° and with different cell thicknesses. As shown in Figure 2c, the CD intensity has a linear relationship to the cell thickness in the range of 0.4–0.9 μm (see inset). This result clearly demonstrates that the CD signal originates from the bulk sample. In addition, the inset suggests that control of the chirality is not possible if the cell is too thin, that is, thinner than 0.3 μm in the present case.

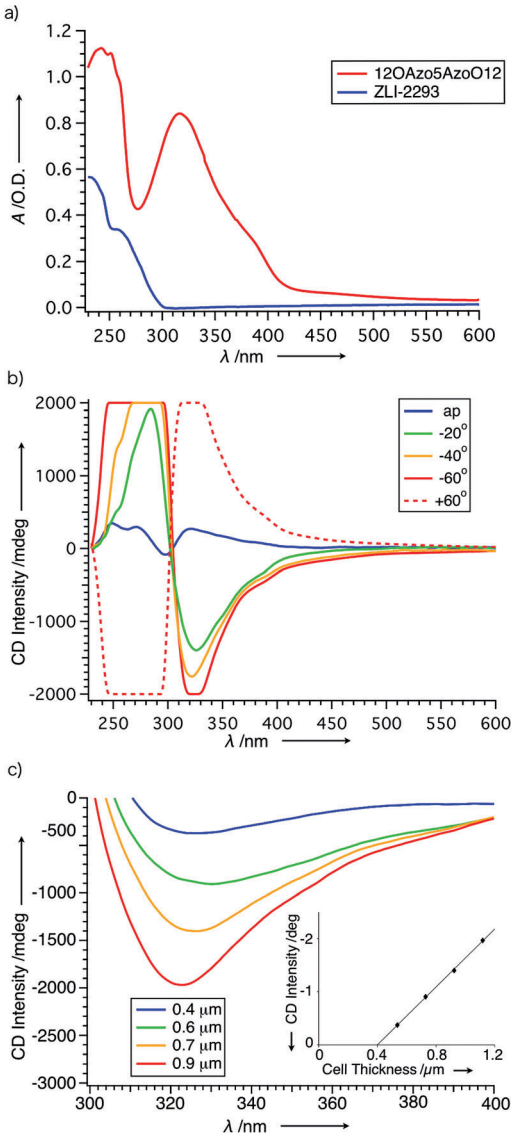

Figure 2. a) UV/Vis absorption spectra of 12OAzo5AzoO12 (bent-core) and ZLI2293 (rod-like). b) CD spectra of the Bx phase made from TN cells of about 0.8 μm thick with various twist angles; antiparallel rubbing (ap; 0°), −20°, −40°, −60°, and +60°. c) CD spectra showing a longer-wavelength peak made from TN cells of various cell thicknesses; 0.4, 0.6, 0.7, and 0.9 μm. The twist angle was fixed at −40°. The inset shows the peak CD intensity as a function of cell thickness.

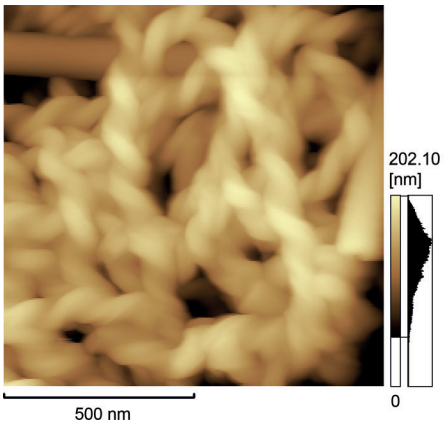

Figure 3. AFM image of Bx surface made from a TN cell with a twist angle of +60° at room temperature taken by a contact mode.

Finally, atomic force microscopy (AFM) was carried out to investigate the relationship between the twist directions of the TN cell and the HNF in the Bx phase. Figure 3 shows the result of AFM of the sample made from a +60° TN cell. All helices in the viewing field are left-handed, no right-handed helices can be seen. On the other hand, a right-handed helix was observed in the sample made from a −60° TN cell. Thus, control of chirality was successfully achieved with almost 100% *ee*. The details of the AFM work will be reported in a separate paper.

It has been reported previously that HNF morphology is preserved even when the B4 material is mixed with mesogens forming nematic, smectic, or columnar phases.[13,29,30] More recently, the B4 phase was reported to exhibit a strong gelation ability for various organic solvents.[31] In other words, the B4 HNFs form a network that acts as a porous nanoconfinement medium and serve as an effective and novel organic nanoconfinement host and gelator.[30] Based on the formation of such a structure in the present mixture we discuss the origin of the CD signal particularly around 280 nm. As mentioned above, by comparing the UV absorption and CD spectra, we can conclude that the longer-wavelength CD signal originates from HNFs of bent-core molecules, whereas the shorter-wavelength one from the rod-like nematic molecules. According to the previous work by Otani et al.,[13] the CD signal corresponding to the chiral contribution of rod-like molecules, which are microphase segregated to the N phase from the HNF (B4) phase, always has the same sign as the CD signal corresponding to the HNFs; the CD signal is always enhanced by the transition from Iso to N of rod-like molecules. The CD signal corresponding to rod-like molecules can be explained by the formation of a superhelical structure.[13,32,33] In the present case, however, the sign of the CD signal corresponding to the rod-like molecules was opposite from that of the signal corresponding to the HNFs. There is a distinct difference between the previous and present systems. In the present case, the CD signal corresponding to the rod-like molecules not only originates from formation of a superhelical structure, but also from formation of a TN structure. It is known that right- and left-handed TN structures give positive and negative CD signals, respectively.[34] We confirmed this behavior by measuring the CD spectra of a simple TN cell (see the Supporting Information, Figure S2). In our definition, right- and left-handed TN structures are made by counterclockwise and clockwise rotations of the rubbing direction on the top surface with respect to the lower surface. From such TN cells, right- and left-handed nanofilaments are generated, and give negative and positive CD signals, respectively; these results are consistent with the AFM and CD measurements. In this way, in the present situation in which TN cells of microphase separated mixtures are used, the TN molecular orientation contributes more to the CD signal than the superhelical structure, probably because the TN orientation suppresses the formation of the superhelical structure to some extent. The

increasing intensity of the CD signal with increasing twist angle of the TN configuration (Figure 2b) is consistent with the conclusion that the TN structure gives the major contribution to the CD signal around 280 nm.

In conclusion, by cooling TN cells we obtained a high excess of homochiral HNF domains in the Bx phase from a mixture having the N–Bx phase sequence. High enantioselectivity was confirmed not only by CD measurements but also by direct observation of HNFs by using AFM. To confirm the generality of this method, CD measurements were also obtained for other two mixtures. As shown in Figure S3 (see the Supporting Information), both mixtures, having the N–Bx transition sequence, show large CD signals, the signs of which correlate with the twist direction of the cells. The origin of CD peaks was studied by comparing UV absorption and CD spectra and by using AFM images. The longer-wavelength peak originates from HNFs in the B4 phase. The shorter-wavelength peak is mainly caused by the TN structure of rod-like molecules, but not by their superhelical structure. This means that the TN structure can be formed even through the gel-like nanoporous networks. Thus, such homochiral networks, which are produced by achiral molecules and geometrical twisted structures, could potentially be used for chiral separations and asymmetric synthesis. These findings could lead to an effective method to produce chiral molecules without the need for any chiral species.

Experimental Section

We made the mixtures listed in Table 1. The mixing ratios were so chosen to exhibit the Iso–N–Bx phase sequence. If the content of rod-shaped molecules is less, other phases such as B2 and other smectic phases appeared between N and Bx. The sample was introduced by capillary in the Iso phase. The cell thickness must be very thin to have an optical density of less than 2. The cell thickness was determined by comparing optical absorbance with that in a standard cell.

For AFM measurements, we first obtained the Bx phase in the same way as in Figure 1. Then we detached one of the glass substrates to expose the free surface of a mixture in the B4 phase. The sample was washed with *n*-hexanes, dried on a hot plate (65 °C), and cooled to room temperature. AFM (Shimadzu, SPM-9600) was used in the tapping mode at room temperature.

Received: January 25, 2013
Published online: May 28, 2013

Keywords: atomic force microscopy · chirality · circular dichroism · helical structures · liquid crystals

[1] L. Pasteur, *Ann. Chim. Phys.* **1848**, *24*, 442.
[2] D. F. Williams, *Biomaterials* **2008**, *29*, 2941.
[3] R. Noyori, *Angew. Chem.* **2002**, *114*, 2108; *Angew. Chem. Int. Ed.* **2002**, *41*, 2008.
[4] P. R. Schreiner, *Chem. Soc. Rev.* **2003**, *32*, 289.
[5] E. Yashima, *J. Chromatogr. A* **2001**, *906*, 105.
[6] T. Niori, T. Sekine, J. Watanabe, T. Furukawa, H. Takezoe, *J. Mater. Chem.* **1996**, *6*, 1231.
[7] H. Takezoe, Y. Takanishi, *Jpn. J. Appl. Phys.* **2006**, *45*, 597.
[8] R. A. Reddy, C. Tschierske, *J. Mater. Chem.* **2006**, *16*, 907.
[9] D. R. Link, G. Natale, R. Shao, J. E. Maclennan, N. A. Clark, E. Korblova, D. M. Walba, *Science* **1997**, *278*, 1924.
[10] H. Niwano, M. Nakata, J. Thisayukta, D. R. Link, H. Takezoe, J. Watanabe, *J. Phys. Chem. B* **2004**, *108*, 14889.
[11] H. Takezoe, *Top. Curr. Chem.* **2012**, *318*, 303.
[12] E. Hough, H. T. Jung, D. Kruerke, M. S. Heberling, M. Nakata, C. D. Jones, D. Chen, D. R. Link, J. Zasadzinski, G. Heppke, J. P. Rabe, W. Stocker, E. Korblova, D. M. Walba, M. A. Glaser, N. A. Clark, *Science* **2009**, *325*, 456.
[13] T. Otani, F. Araoka, K. Ishikawa, H. Takezoe, *J. Am. Chem. Soc.* **2009**, *131*, 12368.
[14] F. Araoka, G. Sugiyama, K. Ishikawa, H. Takezoe, *Opt. Mater. Exp.* **2011**, *1*, 27.
[15] F. Araoka, G. Sugiyama, K. Ishikawa, H. Takezoe, *Adv. Funct. Mater.* **2013**, DOI: 10.1002/adfm.201201889.
[16] W. L. Noorduin, A. A. C. Bode, M. van der Meijden, H. Meekes, A. F. van Etteger, W. J. P. van Enckevort, P. C. M. Christianen, B. Kaptein, R. M. Kellogg, T. Rasing, E. Vlieg, *Nat. Chem.* **2009**, *1*, 729.
[17] F. Vera, J. L. Serrano, M. P. D. Santo, R. Barberi, M. B. Ros, T. Sierra, *J. Mater. Chem.* **2012**, *22*, 18025.
[18] V. Aquilanti, G. S. Maciel, *Orig Life Evol. Biosph.* **2006**, *36*, 435.
[19] N. Micali, H. Engelkamp, P. G. van Rhee, P. C. Christianen, L. Monsu Scolaro, J. C. Maan, *Nat. Chem.* **2012**, *4*, 201.
[20] K. Okano, T. Yamashita, *ChemPhysChem* **2012**, *13*, 2263 – 2271.
[21] T. Miyabe, H. Iida, A. Ohnishi, E. Yashima, *Chem. Sci.* **2012**, *3*, 863.
[22] a) J. Thisayukta, H. Niwano, H. Takezoe, J. Watanabe, *J. Mater. Chem.* **2001**, *11*, 2717; b) F. Araoka, Y. Takanishi, H. Takezoe, A. Kim, B. Park, J. W. Wu, *J. Opt. Soc. Am. B* **2003**, *20*, 314.
[23] K. Shiromo, D. A. Sahade, T. Oda, T. Nihira, Y. Takanishi, K. Ishikawa, H. Takezoe, *Angew. Chem.* **2005**, *117*, 1984; *Angew. Chem. Int. Ed.* **2005**, *44*, 1948.
[24] S.-W. Choi, T. Izumi, Y. Hoshino, Y. Takanishi, K. Ishikawa, J. Watanabe, H. Takezoe, *Angew. Chem.* **2006**, *118*, 1410; *Angew. Chem. Int. Ed.* **2006**, *45*, 1382.
[25] S.-W. Choi, S. Kang, Y. Hoshino, Y. Takanishi, K. Ishikawa, J. Watanabe, H. Takezoe, *Angew. Chem.* **2006**, *118*, 6653; *Angew. Chem. Int. Ed.* **2006**, *45*, 6503.
[26] G. Lee, R. J. Carlton, F. Araoka, N. L. Abbott, H. Takezoe, *Adv. Mater.* **2013**, *25*, 245.
[27] T. Sekine, Y. Takanishi, T. Niori, J. Watanabe, H. Takezoe, *Jpn. J. Appl. Phys.* **1997**, *36*, 6455.
[28] T. Izumi, S. Kang, T. Niori, Y. Takanishi, H. Takezoe, J. Watanabe, *Jpn. J. Appl. Phys.* **2006**, *45*, 1506.
[29] D. Chen, M. S. Heberling, M. Nakata, L. E. Houogh, J. E. Maclennan, M. A. Glaser, E. Korblova, D. M. Walba, N. A. Clark, *ChemPhysChem* **2012**, *13*, 155.
[30] D. Chen, C. Zhu, H. Wang, J. E. Maclennan, M. A. Glaser, E. Korblova, D. M. Walba, J. A. Rego, E. A. Soto-Bustamante, N. A. Clark, *Soft Matter* **2013**, *9*, 462.
[31] A. Zep, M. Salamonczyk, N. Vaupotic, D. Pociecha, E. Gorecka, *Chem. Commun.* **2013**, *49*, 3119.
[32] C. Zhu, D. Chen, Y. Shen, C. D. Jones, M. A. Glaser, J. E. Maclennan, N. A. Clark, *Phys. Rev. E* **2010**, *81*, 011704.
[33] D. Chen, C. Zhu, R. K. Shoemaker, E. Korblova, D. M. Walba, M. A. Glaser, J. E. Maclennan, N. A. Clark, *Langmuir* **2010**, *26*, 15541.
[34] F. D. Saeva, J. J. Wysocki, *J. Am. Chem. Soc.* **1971**, *93*, 5928.

